EurJIC
European Journal of Inorganic Chemistry

Research Article
doi.org/10.1002/ejic.202400322

Chemistry Europe
European Chemical Societies Publishing

www.eurjic.org

Synthesis and Anticancer Properties of Heterobimetallic Fe(II)/Pd(II) Complexes Bearing Different Butadienyl Fragments

Enrica Bortolamiol,[a] Maria Dalla Pozza,[b] Nicola Demitri,[c] Flavio Rizzolio,[a, d] Fabiano Visentin,*[a] Gilles Gasser,*[b] and Thomas Scattolin*[e]

In this work, we describe the synthesis of heterobimetallic Fe(II)/Pd(II) complexes bearing different halides and halide-substituted butadienyl ligands. The synthetic approach involves the preparation of suitable Pd(II)-butadienyl precursors containing a thioquinoline moiety, followed by the substitution of this relatively labile ligand with dppf (dppf = 1,1′-bis(diphenylphosphino)ferrocene). With the exception of complexes containing at least one iodine atom, all compounds were synthesized in high yields and purity, and thoroughly characterized using spectroscopic and diffractometric methods. The investigation of the antiproliferative activity of the synthesized organometallic complexes against ovarian and breast cancer cell lines revealed that all compounds exhibit noteworthy cytotoxicity, with IC_{50} values in the micromolar range and generally comparable to those of cisplatin. Interestingly, significant differences of cytotoxicity among the analysed compounds were observed in the case of MRC-5 normal cells. Of particular interest is the dichloride derivative **3a**, which is essentially inactive towards non-cancerous cells ($IC_{50} > 100$ μM), thus demonstrating promising *in vitro* selectivity that we believe warrants further investigation in the future.

Introduction

Ferrocenyl compounds stand as a fascinating class of organometallic compounds, valued for their unique structural and chemical properties.[1] The structural motif of ferrocene moiety has undoubtedly revolutionized the landscape of organometallic chemistry, opening avenues for diverse applications spanning catalysis, materials science, medicinal chemistry, and beyond.[1–3]

Chemists have leveraged the versatility of ferrocenyl compounds to engineer an impressive array of derivatives, each bearing distinct functional groups or substituents. These modifications not only tailor the physical and chemical properties of ferrocenyl compounds but also endow them with a myriad of applications.

In catalysis, ferrocenyl compounds serve as efficient catalysts for a wide variety of reactions.[4] Their ability to undergo reversible redox processes facilitates electron transfer, enabling catalytic cycles in numerous transformations.[5] From homogeneous catalysis in organic synthesis to heterogeneous catalysis in industrial processes, ferrocenyl compounds have left an indelible mark.[6]

In medicinal chemistry, ferrocenyl compounds and other iron-based derivatives have revealed promising bioactivity profiles. Researchers have explored their potential as anticancer agents, antimicrobial agents, and even as platforms for drug delivery.[3,7] Also in this context, the unique redox behaviour of ferrocene imparts cytotoxicity to cancer cells while sparing healthy tissues, making ferrocenyl-based drugs an intriguing chemotherapeutic option in the fight against cancer.[3,8]

In this vast scenario, heterobimetallic compounds represent a compelling frontier in medicinal chemistry, being able to potentially exploit the synergistic properties of two distinct metal ions to unlock novel therapeutic avenues.[9] These compounds, characterized by the presence of two different metal centers within a single molecule, offer a unique platform for designing targeted and multifunctional agents with enhanced efficacy and selectivity.[10]

[a] Dr. E. Bortolamiol, Prof. Dr. F. Rizzolio, Prof. Dr. F. Visentin
Department of Molecular Sciences and Nanosystems, Università Ca' Foscari, Campus Scientifico Via Torino 155, 30174 Venezia-Mestre, Italy
E-mail: fvise@unive.it

[b] Dr. M. Dalla Pozza, G. Gasser
ChimieParisTech, PSL University, CNRS, Institute of Chemistry for Life and Health Sciences, Laboratory for Inorganic Chemical Biology, 75005, Paris, France
E-mail: gilles.gasser@chimieparistech.psl.eu

[c] Dr. N. Demitri
Area Science Park, Elettra-Sincrotrone Trieste, S.S. 14 Km 163.5, Basovizza, 34149, Trieste, Italy

[d] Prof. Dr. F. Rizzolio
Pathology Unit, Centro di Riferimento Oncologico di Aviano (C.R.O.) IRCCS, via Franco Gallini 2, 33081, Aviano, Italy

[e] Dr. T. Scattolin
Dipartimento di Scienze Chimiche, Università degli Studi di Padova, via Marzolo 1, 35131 Padova, Italy
E-mail: thomas.scattolin@unipd.it

Supporting information for this article is available on the WWW under https://doi.org/10.1002/ejic.202400322

Research Article
doi.org/10.1002/ejic.202400322

At the core of the appeal of heterobimetallic compounds lies their ability to modulate biological processes through finely tuned interactions with biological targets. By judiciously selecting metal ions and coordinating ligands, researchers can potentially tailor the physicochemical properties of these compounds to engage specific biomolecular targets implicated in disease pathology.[9,10]

In particular, one of the primary advantages of heterobimetallic compounds in medicinal chemistry lies in their ability to leverage the complementary properties of different metal ions. For example, the incorporation of transition metal ions with redox-active properties alongside inert or biocompatible metal ions can impart redox-switchable behaviour to the compounds.[9–11] This feature is particularly valuable in the design of agents for targeted drug delivery, where controlled release of therapeutic payloads can be achieved through external stimuli such as changes in pH or the application of electromagnetic fields.[12]

Furthermore, the incorporation of diverse metal ions enables heterobimetallic compounds to exhibit multifunctionality, wherein they can simultaneously modulate multiple biological pathways associated with a particular disease.[9,10] By harnessing the distinct reactivities of different metal centers, researchers can design compounds capable of exerting synergistic effects on complex biological systems, thereby enhancing therapeutic outcomes.[9–11]

The structural diversity afforded by heterobimetallic compounds can further expands their utility in medicinal chemistry. By judiciously selecting bridging ligands and coordinating geometries, researchers can fine-tune the pharmacokinetic and pharmacodynamic properties of these compounds, optimizing their bioavailability, stability, and target specificity.[9]

Finally, In the realm of drug resistance, heterobimetallic compounds offer a promising strategy for overcoming challenges associated with multidrug-resistant pathogens or cancer cells.[9–13] By exploiting the unique mechanisms of action enabled by the synergistic interactions between different metal ions, these compounds can circumvent resistance mechanisms that render conventional monometallic drugs ineffective.[9–11]

In this study, we aimed to combine the well-known biological properties of ferrocenyl compounds with the emerging antitumor properties of organopalladium complexes.[14] In particular, we chose the dppf ligand (dppf = 1,1′-bis(diphenylphosphino)ferrocene) as the ferrocenyl moiety and different halide-substituted Pd(II)-butadienyl fragments. Importantly, the presence of a Pd(II)-butadienyl fragment has recently yielded promising results against various *in vitro*, *ex vivo*, and *in vivo* models of ovarian cancer.[15] In addition, it has been shown that Pd(II)-butadienyl compounds seem to act via an unusual mechanism of action compared to classical palladium-based and platinum-based anticancer agents.

Results and Discussion

Synthesis of Pd(II)-Butadienyl Precursors

The organometallic complexes addressed in this work differ from those recently synthesized and tested in our previous contribution[15] for the presence of a halogen in place of a methyl group in the terminal portion of the butadienyl fragment. This modification has been adopted to evaluate the role of the terminal substituent in the butadienyl fragment on the antiproliferative activity of this fascinating class of organopalladium derivatives. Such a structural modification requires a completely different synthetic protocol compared to the methyl derivatives, which had been obtained by controlled double insertion of dimethylacetylenedicarboxylate (DMA) on a suitable Pd(II)-methyl precursor.[15] In particular, based on some of our recent works,[16] we opted for the addition of stoichiometric amounts of halogens (Cl_2, in the form of $PhICl_2$, Br_2, and I_2) and interhalogens (IBr and ICl) to the palladacyclopentadienyl precursor **1** (Scheme 1). The latter contains a thioquinoline ligand (TMQ) which, besides ensuring the selective formation of (*E,E*)-σ-butadienyl derivatives **2a**–**e**, is easily substitutable by strongly σ-donating ligands such as diphosphines. Notably, the synthesis of complexes **2b**–**e** is already reported in the literature.[16,17]

Another advantage of thioquinoline Pd(II)-butadienyl complexes is the ability to replace iodide or bromide ligands with a chloride via a mild and one-pot process. This metathesis reaction can be achieved without using silver-based dehalogenating agents, but simply by the addition of ICl. Further details on this efficient halide metathesis protocol are reported in our previous work.[17] Following this procedure, we successfully synthesized complex **2f** by reacting complex **2b** with ICl, and subsequently eliminated IBr from the reaction mixture (Schemes 1).

The novel organometallic complexes **2a** and **2f** were thoroughly characterized by ^1H and ^{13}C NMR spectroscopies before being employed as precursors in the next step (see Figures S1–4 in ESI).

In the case of complex **2a**, all proton and carbon signals are significantly shifted compared to the palladacyclopenta-

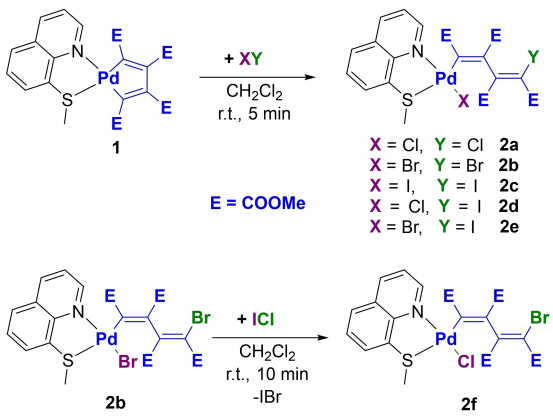

Scheme 1. Synthesis of Pd(II)-butadienyl precursors.

Research Article
doi.org/10.1002/ejic.202400322

dienyl precursor [Pd(TMQ)(C_4(COOMe)$_4$] (**1**). The position of the pyridine proton H^2 is particularly diagnostic (9.72 ppm), as well as the low-fielded resonance of the terminal butadienyl carbon bonded to the halide in the ^{13}C NMR spectrum (129.0 ppm). Moreover, all protons and carbons attributed to the -OCH_3 groups and to the TMQ ligand are easily detectable in the alkyl and aryl regions, respectively. Finally, carbons located in the lowest-field region are ascribable to the carbonyl groups.

In the case of compound **2f**, its ^{1}H NMR spectrum is similar to that of the dibromo derivative **2b**, except for the position of the pyridyl proton H^2 (9.72 ppm vs 9.93 ppm), indicating the successful exchange of the halide. Concerning the ^{13}C NMR analysis, carbon signals are slightly shifted compared to those of compound **2b** and, in particular, the terminal butadienyl carbon bounded to the bromide resonates at 130.6 ppm.

Additionally, the structure of compounds **2a** and **2f** was definitively confirmed through XRD analysis carried out on suitable crystals obtained by slow evaporation of diethyl ether in a dichloromethane solution of the palladium complex (Figure 1).

The crystal data of complexes **2a** and **2f** show the following main bond distances: *i)* Pd–C, ca. 1.99 Å, *ii)* Pd–N, ca. 2.12 Å, *iii)* Pd–Cl, ca. 2.32 Å and *iv)* Pd–S, ca. 2.26 Å. Moreover, the bond angles are compatible with a slightly distorted square planar geometry (C–Pd–Cl, ca. 90°; N–Pd–Cl, ca. 96°; N–Pd–S, ca. 85° and S–Pd–C, ca. 89°). Further details are reported in the experimental section and Electronic Supporting Information (Tables S1, S4 and S5).

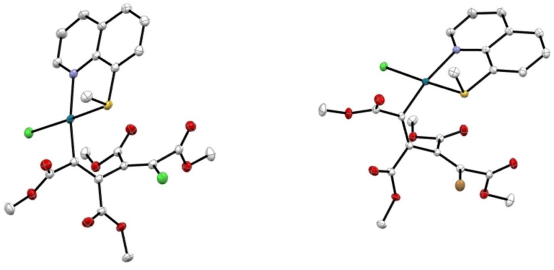

Figure 1. Molecular structures of organometallic complexes **2a** and **2f** are showed with thermal displacement ellipsoids at the 50% probability level. Hydrogen atoms are omitted for clarity.

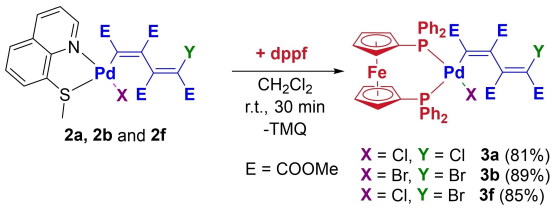

Scheme 2. Synthetic pathway of heterobimetallic Fe(II)/Pd(II) complexes bearing different butadienyl fragments.

Synthesis of Heterobimetallic Fe(II)/Pd(II) Complexes

The target heterobimetallic Fe(II)/Pd(II) complexes were synthesized by addition of one equivalent of the dppf ligand to a dichloromethane solution of the palladium(II)-butadienyl precursors of interest (Scheme 2). The reactions proceeded at room temperature for ca. 30 minutes and, precautionary, under inert atmosphere. Organometallic complexes **3a**, **3b** and **3f** were isolated as yellow powders by precipitation with diethyl ether to remove the TMQ ligand. Unfortunately, in the case of compounds containing at least one iodine atom (**3c**–**e**), many side products can be observed in the isolated solids. The nature of such collateral species is not easily identifiable, and every attempt to purify the target organometallic complexes from by-products has failed. For this reason, compounds **3c**–**e** have not been fully characterized and have therefore been excluded from the study of their antiproliferative activity.

Heterobimetallic Fe(II)/Pd(II) complexes **3a**, **3b**, and **3f** were firstly characterized by NMR spectroscopy (see Figures S5–13 in ESI). In particular, the ^{31}P{^{1}H} NMR spectra, displayed two doublets at 15–17 and 30 ppm with a $J_{P\text{-}P}$ of ca. 18 Hz. Predictably, the phosphorus nucleus *trans* to the halide exhibits the lowest chemical shift.

In the ^{1}H NMR spectra, the eight ferrocenyl protons are present as multiplets at 3.1–6.1 ppm, while the phenyl signals of the phosphine ligand occupy the aromatic region between 7.0 and 8.3 ppm. The four -OCH_3 groups of the butadienyl moiety are identified as singlet peaks between 3.5 and 3.9 ppm. In the ^{13}C{1H} NMR spectra, the methoxy carbons resonate between 51 and 54 ppm, while the ten ferrocenyl signals appear as doublets between 70 and 80 ppm, due to the coupling with phosphorus. In the vinyl and aromatic region (128–145 ppm), other phosphine and butadienyl signals are distinguishable. The four carbonyl carbons resonate between 162 and 168 ppm, featuring three singlets and one doublet. Lastly, the terminal butadienyl carbon bonded to the halide is readily identifiable, exhibiting peaks at 126.4, 118.5, and 118.6 ppm for compounds **3a**, **3b** and **3f**, respectively.

Moreover, in the case of complexes **3b** and **3f**, it was possible to unequivocally confirm their structure by XRD analysis on suitable crystals obtained by slow evaporation of diethylether in a dichloromethane solution of the palladium complex (Figure 2).

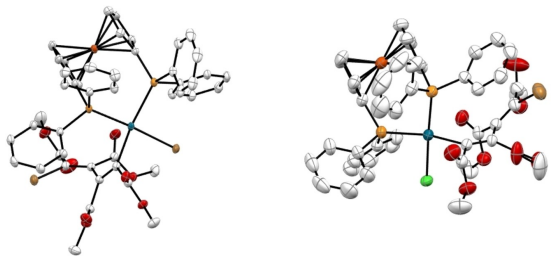

Figure 2. Molecular structures of organometallic complexes **3b** and **3f** are showed with thermal displacement ellipsoids at the 50% probability level. Hydrogen atoms are omitted for clarity.

Research Article
doi.org/10.1002/ejic.202400322

The crystal data of complexes **3b** and **3f** show the following main bond distances: *i)* Pd–C, (2.05–2.06 Å for **3b** and 2.03–2.05 for **3f**), *ii)* Pd–P, (2.38–2.41 Å and 2.28–2.29 Å for **3b** and 2.37–2.39 Å and 2.27–2.28 Å for **3f**), *iii)* Pd–Cl, ca. 2.38 Å for **3f** and *iv)* Pd–Br, ca. 2.47 Å for **3b**. Moreover, the bond angles are compatible with a slightly distorted square planar geometry (C–Pd-Br, 84–86° for **3b**; P–Pd-Br, 85–87° for **3b**; C–Pd–Cl, 85–87° for **3f**; P–Pd–Cl, 85–87° for **3f**; P–Pd-P, 96–98° for both complexes and P–Pd–C, ca. 90° for both complexes. Therefore, the bite angle of dppf (ca. 97°) is scarcely influenced by the nature of coordinated halide (bromide or chloride). Further details are reported in the experimental section and Electronic Supporting Information (Tables S1–3 and S6–7).

For the sake of completeness, the IR (KBr pellets) and UV-Vis (in $CHCl_3$) spectra of complexes **3a**, **3b** and **3f** are also reported in the Electronic Supporting Information (Figures S14–19).

Antiproliferative Activity on Cancer and Normal Cell Lines

The antiproliferative activity of the synthesized heterobimetallic Fe(II)/Pd(II) complexes was evaluated on four high-serous ovarian cancer cell lines (OVSHAO, SKOV-3, OVCAR-5 and KURAMOCHI) and MDA-MB-231 triple-negative breast cancer cells. The antiproliferative activity, expressed as IC_{50} values (μM), was compared with that of cisplatin, which, besides being a reference metallodrug, is also commonly included in the first line of treatment of ovarian cancer (Table 1). Moreover, all organometallic complexes were tested towards MRC-5 non-cancerous cells (human lung fibroblasts) to verify the potential selectivity of these heterobimetallic derivatives towards cancer cells.

All compounds are characterized by an antiproliferative activity in the micromolar concentration range, and their cytotoxicity was generally comparable to that of cisplatin in all cancer cell lines.

The IC_{50} values were similar for the three compounds within the various cancer cell lines, with no significant IC_{50} variations resulting from the different halogens decorating the complexes. Notably, the cytotoxicity against SKOV-3 was remarkably lower compared to the other three high-grade serous ovarian cancer (HGSOC) cell lines (OVSHAO, OVCAR-5, KURAMOCHI), especially for compound **3a**.

Table 1. IC_{50} values (μM) of heterobimetallic Fe(II)/Pd(II) complexes and cisplatin for cancer (OVSHAO, SKOV-3, OVCAR-5, KURAMOCHI, MDA-MB-231) and normal (MRC-5) cell lines.

	Cisplatin	3a	3b	3f
OVSHAO	0.6 ± 0.1	1.2 ± 0.1	2.0 ± 0.3	2.9 ± 0.5
SKOV-3	3.1 ± 0.2	31 ± 3	16 ± 3	12 ± 3
OVCAR-5	0.44 ± 0.09	5 ± 1	4.5 ± 0.3	5.3 ± 0.4
KURAMOCHI	1.25 ± 0.08	4.0 ± 0.5	2.1 ± 0.1	2.6 ± 0.2
MDA-MB-231	36.3 ± 0.8	7.1 ± 0.7	9.3 ± 0.4	8 ± 1
MRC-5	1.52 ± 0.08	> 100	20 ± 9	31 ± 5

Data after 96 h of incubation. Stock solutions in DMSO for all complexes; stock solutions in H_2O/NaCl for cisplatin.

On the other hand, our heterobimetallic Fe(II)/Pd(II) complexes exhibited a higher cytotoxicity than cisplatin against triple-negative breast cancer cells (MDA-MB-231). Notably, in a very recent study of our group,[18] we demonstrated that butadienyl complexes containing two triphenylphosphine ligands instead of dppf are inactive ($IC_{50} > 100$ μM) towards triple-negative breast cancer cells, regardless of the nature of the halide bound to the metal center and to the terminal carbon of the butadienyl fragment.

The results concerning MRC-5 non-cancerous cells shed light on the importance of having at least one chlorine atom in the structure of the tested complexes. Indeed, complexes **3a** and **3f** showed the lowest cytotoxicity towards non-cancerous cells, with the former being substantially inactive ($IC_{50} > 100$ μM). The high selectivity towards cancer cells observed *in vitro* for the heterobimetallic Fe(II)/Pd(II) complex **3a** makes this derivative particularly attracting and worthy of further investigation in the future.

Conclusions

In this work, we describe the preparation of novel heterobimetallic Fe(II)/Pd(II) complexes containing different halides and halide-substituted butadienyl ligands. More in detail, the target complexes were obtained by reacting Pd(II)-butadienyl precursors bearing the TMQ thioquinoline ligand, followed by substitution of this NS moiety with dppf (dppf = 1,1′-bis(diphenylphosphino)ferrocene) as ferrocenyl unit. Except for organometallic complexes containing at least one iodine atom, all compounds were obtained in high yields and purity, and thoroughly characterized by NMR and XRD analyses.

The synthesized heterobimetallic Fe(II)/Pd(II) complexes were tested as potential anticancer agents towards five different ovarian (SKOV-3, OVSHAO, OVCAR-5, KURAMOCHI) and breast cancer (MDA-MB-231) cell lines, showing significant cytotoxicity, with IC_{50} values in the micromolar range. Notably, the IC_{50} values are generally comparable to those of cisplatin.

The greatest difference among the tested compounds was observed in MRC-5 non-cancerous cells. In particular, the presence of at least one chlorine atom seems crucial for reducing cytotoxicity towards non-cancerous cells. In this respect, the dichloride derivative **3a** is particularly interesting since it shows a negligible activity against non-cancerous cells ($IC_{50} > 100$ μM), and therefore an *in vitro* selectivity towards cancer ones.

We strongly believe that the interesting results obtained with this compound deserve further investigation from a biological point of view, especially the evaluation of its cytotoxicity in *ex vivo* and *in vivo* models, as well as the detailed study of its mechanism of action. Such studies are currently ongoing in our laboratories.

Research Article
doi.org/10.1002/ejic.202400322

Experimental

Materials and Methods

Dichloromethane and diethyl ether were anhydrified under molecular sieves (4 Å, 10 %) and maintained under Argon atmosphere. Iodine monochloride and 1,1′-bis(diphenylphosphino)ferrocene were used as purchased (Sigma-Aldrich). Complexes **1**,[16b] **2b-e**[16b,17] and iodobenzene dichloride were synthesized following the published procedures.[19]

NMR spectra were obtained by Bruker 300 MHz spectrometer.

IR spectra (KBr) were recorded on a Perkin – Elmer Spectrum One spectrophotometer.

Elemental analyses were carried out using an Elemental CHN 'CUBO Micro Vario' analyzer.

UV-Vis spectra were recorded on a Lambda 40 UV/Vis spectrophotometer.

Synthesis of [PdCl(TMQ)(C_4(COOMe)$_4$Cl] (2a). To a solution of complex **1** (0.1013 g, 0.1791 mmol) in 10 mL of anhydrous CH_2Cl_2, a solution of iodobenzene dichloride (0.0493 g, 0.1791 mmol) in 4 mL of dichloromethane was added under inert atmosphere (Ar). The resulting solution was stirred at room temperature for 10 minutes, filtered through a Millipore apparatus and concentrated under vacuum. From the concentrated solution, the title complex was precipitated by addition of diethyl ether and filtered on a sintered glass filter. 0.1096 g (yield 96 %) of **2a** was isolated as a yellow powder.

^{1}H NMR (300 MHz, $CDCl_3$, T = 298 K, ppm) δ: 3.02 (s, 3H, SCH_3), 3.73 (s, 3H, OCH_3), 3.75 (s, 3H, OCH_3), 3.84 (s, 3H, OCH_3), 3.87 (s, 3H, OCH_3), 7.64 (dd, 1H, J = 8.3, 5.0 Hz, H^3), 7.74 (dd, 1H, J = 8.2, 7.4 Hz, H^6), 8.02 (d, 1H, J = 8.1 Hz, H^5), 8.10 (d, 1H, J = 6.7 Hz, H^7), 8.43 (dd, 1H, J = 8.4, 1.3 Hz, H^4), 9.72 (dd, 1H, J = 5.0, 1.4 Hz, H^2).

^{13}C{^{1}H} NMR ($CDCl_3$, T = 298 K, ppm) δ: 28.9 (CH_3, SCH_3), 52.4 (CH_3, OCH_3), 52.5 (CH_3, OCH_3), 53.4 (CH_3, OCH_3), 53.5 (CH_3, OCH_3), 123.4 (CH, C^3), 128.4 (CH, C^6), 129.0 (C, CCl), 130.5 (C, C^{10}), 130.7 (CH, C^5), 133.3 (C, C^8), 134.9 (CH, C^7), 137.8 (C, C═C), 138.4 (C, C═C),139.6 (CH, C^4), 147.3 (C, C^9), 153.2 (CH, C^2), 160.7 (C, C═C C═O), 163.6 (C, C═O), 166.2 (C, C═O), 172.4 (C, C═O).

Synthesis of [PdCl(TMQ)(C_4(COOMe)$_4$Br] (2f). To a solution of complex **2b** (0.0880 g, 0.1213 mmol) in 6 mL of anhydrous CH_2Cl_2, a solution of ICl (0.0237 g, 0.1460 mmol) in 4 mL of dichloromethane was quickly added under inert atmosphere (Ar). The resulting red solution was stirred at room temperature for 7 minutes and dried under vacuum. 2 mL of CH_2Cl_2 was added and the title complex was precipitated by addition of 3.5 mL of diethyl ether. 0.0624 g (yield 75 %) of **2f** (pale-yellow) was isolated by filtration on a sintered glass filter.

^{1}H NMR (300 MHz, $CDCl_3$, T = 298 K, ppm) δ: 3.04 (s, 3H, SCH_3), 3.73 (s, 3H, OCH_3), 3.74 (s, 3H, OCH_3), 3.85 (s, 3H, OCH_3), 3.88 (s, 3H, OCH_3), 7.63 (dd, 1H, *J* = 8.3, 5.0 Hz, H^3), 7.75 (dd, 1H, *J* = 8.2, 7.4 Hz, H^6), 8.02 (dd, 1H, *J* = 8.1, 1.1 Hz, H^5), 8.11 (d, 1H, *J* = 7.4, 1.1 Hz, H^7), 8.43 (dd, 1H, *J* = 8.4, 1.5 Hz, H^4), 9.72 (dd, 1H, *J* = 5.0, 1.6 Hz, H^2).

^{13}C{^{1}H} NMR ($CDCl_3$, T = 298 K, ppm) δ: 29.0 (CH_3, SCH_3), 52.3 (CH_3, OCH_3), 52.4 (CH_3, OCH_3), 53.5 (CH_3, OCH_3), 53.6 (CH_3, OCH_3), 123.3 (CH, C^3), 128.3 (CH, C^6), 130.4 (C, C^{10}), 130.6 (C, CBr), 130.7 (CH, C^5), 133.3 (C, C^8), 134.9 (CH, C^7), 140.4 (C, C═C),139.6 (CH, C^4), 147.3 (C, C^9), 153.2 (CH, C^2), 157.8 (C, C═C), 159.1 (C, C═C), 160.4 (C, C═O), 164.4 (C, C═O), 166.0 (C, C═O), 172.3 (C, C═O).

Synthesis of [PdCl(dppf)(C_4(COOMe)$_4$Cl] (3a). To a solution of complex **2a** (0.0699 g, 0.1098 mmol) in 10 mL of anhydrous CH_2Cl_2, a solution of 0.0753 g (0.1318 mmol) 1,1′-bis(diphenylphosphino)ferrocene (dppf) in 5 mL of CH_2Cl_2 was added under inert atmosphere (Ar). The resulting orange solution was stirred at room temperature for 30 minutes, filtered through a Millipore apparatus and concentrated under vacuum. From the concentrated solution, the title complex was precipitated by addition of 15 mL of diethyl ether and filtered on a sintered glass filter. 0.0902 g (yield 81 %) of **3a** was obtained as a pale orange powder.

^{1}H NMR ($CDCl_3$, T = 298 K, ppm) δ = 3.16–3.19 (m, 1H, Fc–H), 3.51 (s, 3H, OCH_3), 3.47–3.50 (m, 1H, Fc–H), 3.71 (s, 3H, OCH_3), 3.82 (s, 3H, OCH_3), 3.86 (s, 3H, OCH_3), 4.01–4.06 (m, 1H, Fc–H), 4.07–4.10 (m, 1H, Fc–H), 4.26–4.29 (m, 1H, Fc–H), 4.29–4.32 (m, 1H, Fc–H), 4.74–4.79 (m, 1H, Fc–H), 6.06 (bs, 1H, Fc–H), 7.08 (td, *J* = 7.9, 2.2 Hz, 2H, Ar–H), 7.13–7.27 (m, 4H, Ar–H), 7.32–7.45 (m, 6H, Ar–H), 7.46–7.59 (m, 3H, Ar–H), 7.76 (dd, *J* = 12.7, 7.4 Hz, 2H, Ar–H), 7.84–7.96 (bm, 1H, Ar–H), 8.20–8.29 (m, 2H, Ar–H).

^{31}P{^{1}H} NMR ($CDCl_3$, T = 298 K, ppm) δ = 17.2 (d, $J_{P\text{-}P}$ = 17.9 Hz), 30.8 (d, $J_{P\text{-}P}$ = 17.9 Hz).

^{13}C{^{1} H} NMR ($CDCl_3$, T = 298 K, ppm) δ = 51.7 (CH_3, OCH_3), 52.0 (CH_3, OCH_3), 53.5 (CH_3, OCH_3), 54.1 (CH_3, OCH_3), 70.6 (CH, d, $J_{C\text{-}P}$ = 4.7 Hz, Fc-CH), 72.1 (CH, d, $J_{C\text{-}P}$ = 5.4 Hz, Fc-CH), 73.4 (CH, d, $J_{C\text{-}P}$ = 5.6 Hz, Fc-CH), 73.6 (C, dd, $J_{C\text{-}P}$ = 44.5, 3.4 Hz, Fc–C), 73.6 (CH, d, $J_{C\text{-}P}$ = 10.4 Hz, Fc-CH), 75.5–75.8 (CH, Fc-CH), 78.7 (C, dd, $J_{C\text{-}P}$ = 55.9, 7.9 Hz, Fc–C), 79.5 (CH, d, $J_{C\text{-}P}$ = 21.1 Hz, Fc-CH), 126.4 (C, CCl), 127.7–128.2 (CH, Ar-CH), 128.6 (CH, d, $J_{C\text{-}P}$ = 9.6 Hz, Ar-CH), 129.9 (C, d, $J_{C\text{-}P}$ = 3.8 Hz, C═C), 130.0 (C, d, $J_{C\text{-}P}$ = 3.8 Hz, C═C), 130.1 (CH, d, $J_{C\text{-}P}$ = 2.3 Hz, Ar-CH), 130.3 (CH, d, $J_{C\text{-}P}$ = 2.8 Hz, Ar-CH), 131.0 (CH, d, $J_{C\text{-}P}$ = 2.1 Hz, Ar-CH), 131.3–132.1 (C, Ar–C), 132.3 (C, d, $J_{C\text{-}P}$ = 56.0 Hz, *ipso*-Ar–C), 132.4 (C, d, $J_{C\text{-}P}$ = 44.9 Hz, *ipso*-Ar–C), 133.6 (CH, d, $J_{C\text{-}P}$ = 10.3 Hz, Ar-CH), 135.5 (C, d, $J_{C\text{-}P}$ = 55.0 Hz, *ipso*-Ar–C), 136.3–136.9 (CH, Ar-CH), 140.9 (C, d, $J_{C\text{-}P}$ = 5.9 Hz, C═C), 162.8 (C, C═O), 164.4 (C, d, $J_{C\text{-}P}$ = 16.0 Hz, C═O), 167.5 (C, C═O), 172.0 (C, C═O).

Elemental analysis calcd (%) for $C_{46}H_{40}Cl_2FeO_8P_2Pd$: C, 54.38; H, 3.97; found: C, 54.09, H, 4.11.

Synthesis of [PdBr(dppf)(C_4(COOMe)$_4$Br] (3b). To a solution of complex **2b** (0.0897 g, 0.1236 mmol) in 10 mL of anhydrous CH_2Cl_2, a solution of 0.0808 g (0.1457 mmol) 1,1′-bis(diphenylphosphino)ferrocene (dppf) in 5 mL of CH_2Cl_2 was added under inert atmosphere (Ar). The resulting orange solution was stirred at room temperature for 30 minutes, filtered through a Millipore apparatus and concentrated under vacuum. From the concentrated solution, the title complex was precipitated by addition of diethyl ether and filtered on a sintered glass filter. 0.1222 g (yield 89 %) of **3b** was obtained as a yellow powder.

^{1}H NMR ($CDCl_3$, T = 298 K, ppm) δ = 3.07–3.10 (m, 1H, Fc–H), 3.52 (s, 3H, OCH_3), 3.53–3.56 (m, 1H, Fc–H), 3.71 (s, 3H, OCH_3), 3.81 (s, 3H, OCH_3), 3.83 (s, 3H, OCH_3), 4.00–4.03 (m, 1H, Fc–H), 4.07–4.10 (m, 1H, Fc–H), 4.30–4.33 (m, 2H, Fc–H), 4.76–4.79 (m, 1H, Fc–H), 6.07 (bs, 1H, Fc–H), 7.05 (td, *J* = 7.9, 2.2 Hz, 2H, Ar–H), 7.15–7.25 (m, 4H, Ar–H), 7.32–7.45 (m, 6H, Ar–H), 7.46–7.59 (m, 3H, Ar–H), 7.72–7.81 (m, 2H, Ar–H), 7.86–7.94 (bm, 1H, Ar–H), 8.19–8.27 (m, 2H, Ar–H).

^{31}P{^{1}H} NMR ($CDCl_3$, T = 298 K, ppm) δ = 15.1 (d, $J_{P\text{-}P}$ = 17.8 Hz), 30.0 (d, $J_{P\text{-}P}$ = 17.8 Hz).

^{13}C{^{1} H} NMR ($CDCl_3$, T = 298 K, ppm) δ = 51.7 (CH_3, OCH_3), 52.1 (CH_3, OCH_3), 53.6 (CH_3, OCH_3), 54.1 (CH_3, OCH_3), 70.6 (CH, d, $J_{C\text{-}P}$ = 4.4 Hz, Fc-CH), 72.2 (CH, d, $J_{C\text{-}P}$ = 4.4 Hz, Fc-CH), 73.3 (CH, d, $J_{C\text{-}P}$ = 5.6 Hz, Fc-CH), 73.5 (CH, d, $J_{C\text{-}P}$ = 10.4 Hz, Fc-CH), 74.3 (C, dd, $J_{C\text{-}P}$ = 43.7, 3.8 Hz, Fc–C), 75.5–75.7 (CH, Fc-CH), 78.5 (C, dd, $J_{C\text{-}P}$ = 54.2, 7.4 Hz, Fc–C), 79.5 (CH, d, $J_{C\text{-}P}$ = 22.2 Hz, Fc-CH), 118.5 (C, CBr), 127.8 (CH, d, $J_{C\text{-}P}$ = 3.7 Hz, Ar-CH), 127.9 (CH, d, $J_{C\text{-}P}$ = 2.8 Hz, Ar-CH), 128.1 (CH, d, $J_{C\text{-}P}$ = 11.0 Hz, Ar-CH), 128.4 (CH, d, $J_{C\text{-}P}$ = 9.7 Hz, Ar-CH), 130.0 (CH, d, $J_{C\text{-}P}$ = 2.1 Hz, Ar-CH), 130.3 (CH, d, $J_{C\text{-}P}$ = 2.6 Hz, Ar-CH), 130.9 (CH, d, $J_{C\text{-}P}$ = 2.3 Hz, Ar-CH),

Research Article
doi.org/10.1002/ejic.202400322

131.5 (C, d, $J_{C\text{-}P}$ = 38.6 Hz, *ipso*-Ar–C), 131.6 (CH, d, $J_{C\text{-}P}$ = 4.5 Hz, Ar-CH), 131.7 CH, d, $J_{C\text{-}P}$ = 2.2 Hz, Ar-CH), 132.9 (C, d, $J_{C\text{-}P}$ = 54.4 Hz, *ipso*-Ar–C), 133.8 (CH, d, $J_{C\text{-}P}$ = 10.3 Hz, Ar-CH), 133.8 (C, d, $J_{C\text{-}P}$ = 45.9 Hz, *ipso*-Ar–C), 135.1 (C, $J_{C\text{-}P}$ = 3.4 Hz, C=C),135.2 (C, $J_{C\text{-}P}$ = 6.1 Hz, C=C), 135.3 (C, d, $J_{C\text{-}P}$ = 53.4 Hz, *ipso*-Ar–C), 136.6 (CH, d, $J_{C\text{-}P}$ = 14.5 Hz, Ar-CH), 137.1 (CH, d, $J_{C\text{-}P}$ = 11.4 Hz, Ar-CH), 143.4 (C, C=C), 143.5 (C, $J_{C\text{-}P}$ = 6.0 Hz, C=C), 163.3 (C, C=O), 164.2 (C, d, $J_{C\text{-}P}$ = 15.6 Hz, C=O), 167.6 (C, C=O), 172.2 (C, C=O).

Elemental analysis calcd (%) for $C_{46}H_{40}Br_2FeO_8P_2Pd$: C, 50.01; H, 3.65; found: C, 50.38, H, 3.54.

Synthesis of [PdCl(dppf)(C_4(COOMe)$_4$Br] (3f). To a solution of complex **2f** (0.0525 g, 0.0771 mmol) in 8 mL of anhydrous CH_2Cl_2, a solution of 0.0480 g (0.0869 mmol) 1,1′-bis(diphenylphosphino)ferrocene (dppf) in 2 mL of CH_2Cl_2 was added under inert atmosphere (Ar). The resulting dark yellow solution was stirred at room temperature for 40 minutes, filtered through a Millipore apparatus and the solvent was removed under vacuum. The title complex was precipitated from a dichloromethane/diethylether solution (1.5 mL/3 mL) and filtered on a sintered glass filter. 0.0697 g (yield 85%) of **3f** was obtained as a yellow powder.

^{1}H NMR ($CDCl_3$, T = 298 K, ppm) δ = 3.11–3.15 (m, 1H, Fc–H), 3.48–3.51 (m, 1H, Fc–H), 3.53 (s, 3H, OCH_3), 3.72 (s, 3H, OCH_3), 3.82 (s, 3H, OCH_3), 3.84 (s, 3H, OCH_3), 4.02–4.05 (m, 1H, Fc–H), 4.06–4.11 (m, 1H, Fc–H), 4.29–4.34 (m, 2H, Fc–H), 4.74–4.80 (m, 1H, Fc–H), 6.01 (bs, 1H, Fc–H), 7.02–7.11 (m, 2H, Ar–H), 7.15–7.27 (m, 4H, Ar–H), 7.34–7.45 (m, 6H, Ar–H), 7.47–7.58 (m, 3H, Ar–H), 7.74 (dd, *J* = 13.0, 7.8 Hz, 2H, Ar–H), 7.82–7.95 (br, 1H, Ar–H), 8.20–8.29 (m, 2H, Ar–H).

^{31} P{^{1}H} NMR ($CDCl_3$, T = 298 K, ppm) δ = 17.1 (d, $J_{P\text{-}P}$ = 17.6 Hz), 30.7 (d, $J_{P\text{-}P}$ = 17.6 Hz).

^{13}C{^{1} H} NMR ($CDCl_3$, T = 298 K, ppm) δ = 51.7 (CH_3, OCH_3), 52.0 (CH_3, OCH_3), 53.6 (CH_3, OCH_3), 54.0 (CH_3, OCH_3), 70.7 (CH, d, $J_{C\text{-}P}$ = 4.2 Hz, Fc-CH), 72.2 (CH, d, $J_{C\text{-}P}$ = 4.2 Hz, Fc-CH), 73.4 (CH, d, $J_{C\text{-}P}$ = 5.4 Hz, Fc-CH), 73.5 (C, dd, $J_{C\text{-}P}$ = 44.5, 2.9 Hz, Fc–C), 73.6 (CH, d, $J_{C\text{-}P}$ = 10.2 Hz, Fc-CH), 75.5–75.7 (CH, Fc-CH), 78.7 (C, dd, $J_{C\text{-}P}$ = 55.8, 7.6 Hz, Fc–C), 79.8 (CH, d, $J_{C\text{-}P}$ = 21.0 Hz, Fc-CH), 118.6 (C, CBr), 127.9 (CH, d, $J_{C\text{-}P}$ = 9.6 Hz, Ar-CH), 128.0 (CH, d, $J_{C\text{-}P}$ = 5.6 Hz, Ar-CH), 128.1 (CH, d, $J_{C\text{-}P}$ = 8.2 Hz, Ar-CH), 128.5 (CH, d, $J_{C\text{-}P}$ = 9.7 Hz, Ar-CH), 130.1 (CH, d, $J_{C\text{-}P}$ = 2.5 Hz, Ar-CH), 130.4 (CH, d, $J_{C\text{-}P}$ = 2.8 Hz, Ar-CH), 130.9 (CH, Ar-CH), 131.1 (C, C=C), 131.2 (C, C=C), 130.1–133.0 (C, Ar–C) 133.6–134.2 (CH, Ar-CH), 135.2 (C, d, $J_{C\text{-}P}$ = 54.6 Hz, *ipso*-Ar–C), 136.4–136.8 (CH, Ar-CH), 143.2 (C, d, $J_{C\text{-}P}$ = 6.9 Hz, C=C), 143.3 (C, d, $J_{C\text{-}P}$ = 6.9 Hz, C=C), 163.4 (C, C=O), 164.0 (C, d, $J_{C\text{-}P}$ = 15.5 Hz, C=O), 167.8 (C, C=O), 172.0 (C, C=O).

Elemental analysis calcd (%) for $C_{46}H_{40}BrClFeO_8P_2Pd$: C, 52.10; H, 3.80; found: C, 51.82, H, 3.91.

Antiproliferative Activity

Five cancer cells lines (OVSHAO, SKOV-3, OVCAR-5, KURAMOCHI and MDA-MB-231) and one non-tumoral cell type (MRC-5) were employed and grown in accordance with the supplier's instructions and maintained at 37 °C in humidified atmosphere with 5% of CO_2. Cells were seeded in 96 well and treated after 24 h of incubation with increasing concentration of heterobimetallic Fe(II)/Pd(II) complexes (0.001, 0.01, 0.1, 1, 10, 100 μM). After 96 h of drug treatment, cell viability was measured with a CellTiter glow assay (Promega, Madison, WI, USA) with BioTek Synergy H1. IC_{50} values were calculated from logistical dose response curves and were obtained as average values from experiments in triplicates.

Crystal Structure Determination

2a, **2f**, **3b** and **3f** crystals data were collected at XRD2 beamline of the Elettra Synchrotron, Trieste (Italy),[20] using a monochromatic wavelength of 0.620 Å, at 100 K or 298 K. The data sets were integrated, scaled and corrected for Lorentz, absorption and polarization effects using XDS package.[21] Data from two random orientations have been merged to obtain complete datasets for **3f** polymorphs (triclinic α and monoclinic β), using CCP4-Aimless[22,23] and for triclinic β-**3b** using SADABS code. Two independent **3b** polymorphs have been found in the same batch (trigonal α and triclinic β packing). The structures were solved by direct methods using SHELXT program[24] and refined using full − matrix least − squares implemented in SHELXL − 2018/3.[25] Thermal motions for all non − hydrogen atoms have been treated anisotropically and hydrogens have been included at calculated positions, riding on their carrier atoms. Heavily disordered solvent contributions have been removed with Platon SQUEEZE[26] routine in **3b** crystal forms (corresponding to ~1 chloroform molecule in polymorph α and ~1 diethyl ether molecule in polymorph β, for each **3b** molecule). Minor geometric and thermal restrains (DFIX, DANG, FLAT and SIMU) have been used to properly model disordered and poorly defined fragments. The Coot program was used for structure building.[27] Pictures were prepared using Ortep3[28] and Pymol[29] software.

Deposition Numbers "https://www.ccdc.cam.ac.uk/services/structures?id=doi:10.1002/ejic.202400322" 2333037 and 2333038 (for **3b**, polymorph α, 100 K), 2333035 (for **3b**, polymorph β, 100 K), 2333031 and 2333033 (for **2f**, 100 K and 298 K), 2333032 (for **2a**, 100 K), 2333034 (for **3f**, polymorph α, 298 K), 2333036 (for **3f**, polymorph β, 100 K), contain the supplementary crystallographic data for this paper. These data are provided free of charge by the joint Cambridge Crystallographic Data Centre and Fachinformationszentrum Karlsruhe "http://www.ccdc.cam.ac.uk/structures" Access Structures service.

Acknowledgements

FR was financially supported by Fondazione AIRC per la Ricerca sul Cancro (Grant AIRC IG23566). We are grateful for financial support from the European Union's Horizon 2020 research and innovation programme (Marie Skłodowska-Curie grant agreement No. 861381), the ERC Consolidator Grant PhotoMedMet to G.G. (GA 681679), the program "Investissements d' Avenir" launched by the French Government and implemented by the ANR with the reference ANR-10-IDEX-0001–02 PSL (G.G.). Open Access publishing facilitated by Università degli Studi di Padova, as part of the Wiley - CRUI-CARE agreement.

Conflict of Interests

The authors declare no conflict of interest.

Data Availability Statement

The data that support the findings of this study are available in the supplementary material of this article.

Keywords: Heterobimetallic complexes · Palladium complexes · Ferrocenyl compounds · Butadienyl ligands · Anticancer activity

[1] P. Stepnicka , *Ferrocenes: Ligands, Materials and Biomolecules*, J. Wiley & Sons, **2008**.
[2] a) T. J. Kealy, P. L. Pauson, *Nature* **1951**, *168*, 1039–1040; b) S. A. Miller, J. A. Tebboth, J. F. Tremaine, *J. Chem. Soc.* **1952**, 632–635; c) G. Wilkinson, M. Rosenblum, M. C. Whiting, R. B. Woodward, *J. Am. Chem. Soc.* **1952**, *74*, 2125–2126; d) W. Pfab, E. O. Fischer, *Z. Anorg. Allg. Chem.* **1953**, *274*, 316–322.
[3] a) M. Patra, G. Gasser, *Nat. Chem. Rev.* **2017**, *1*, 0066; b) S. S. Braga, A. M. S. Silva, *Organometallics* **2013**, *32*, 5626–5639; c) C. Ornelas, *New J. Chem.* **2011**, *35*, 1973–1985; d) D. R. van Staveren, N. Metzler-Nolte, *Chem. Rev.* **2004**, *104*, 5931–5985.
[4] a) R. Atkinson, V. C. Gibson, N. J. Long, *Chem. Soc. Rev.* **2004**, *33*, 313–328; b) J. Wei, P. L. Diaconescu, *Acc. Chem. Res.* **2019**, *52*, 415–424.
[5] D. Astruc, *Eur. J. Inorg. Chem.* **2016**, *2017*, 6–29.
[6] F. A. Larik, A. Saeed, T. A. Fattah, U. Muqadar, P. A. Channar, *Appl. Organomet. Chem.* **2017**, *31*, e3664.
[7] a) C. Biot, G. Glorian, L. A. Maciejewski, J. Brocard, *J. Med. Chem.* **1997**, *40*, 3715–3718; b) O. Domarle, G. Blampain, H. Agnaniet, T. Nzadiyabi, J. Lebibi, J. Brocard, L. Maciejewski, C. Biot, A. J. Georges, P. Millet, *Antimicrob. Agents Chemother.* **1998**, *42*, 540–544; c) T. Sarkar, A. Bhattacharyya, S. Banerjee, A. Hussain, *Chem. Commun.* **2020**, *56*, 7981–7984; d) S. B. Chanu, S. Banerjee, M. Roy, *Eur. J. Med. Chem.* **2017**, *125*, 816–824; e) T. Sarkar, S. Banerjee, A. Hussain, *RSC Adv.* **2015**, *5*, 29276–29284.
[8] a) S. Top, J. Tang, A. Vessières, D. Carrez, C. Provot, G. Jaouen, *Chem. Commun.* **1996**, 955–956; b) Q. Michard, G. Jaouen, A. Vessieres, B. A. Bernard, *J. Inorg. Biochem.* **2008**, *102*, 1980–1985; c) A. Citta, A. Folda, A. Bindoli, P. Pigeon, S. Top, A. Vessières, M. Salmain, G. Jaouen, M. P. Rigobello, *J. Med. Chem.* **2014**, *57*, 8849–8859; d) C. Bruyère, V. Mathieu, A. Vessières, P. Pigeon, S. Top, G. Jaouen, R. Kiss, *J. Inorg. Biochem.* **2014**, *141*, 144–151.
[9] a) E. J. Anthony, E. M. Bolitho, H. E. Bridgewater, O. W. L. Carter, J. M. Donnelly, C. Imberti, E. C. Lant, F. Lermyte, R. J. Needham, M. Palau, P. J. Sadler, H. Shi, F.-X. Wang, W. Zhang, Z. Zhang, *Chem. Sci.* **2020**, *11*, 12888–12917; b) G. Gasser, I. Ott, N. Metzler-Nolte, *J. Med. Chem.* **2011**, *54*, 3–25; c) P. Zhang, P. J. Sadler, *J. Organomet. Chem.* **2017**, *839*, 5–14; d) T. Scattolin, A. A. Logvinov, N. V. Tzouras, C. S. J. Cazin, S. P. Nolan, *Organometallics* **2023**, *42*, 2692–2730; e) E. Bortolamiol, F. Visentin, T. Scattolin, *Appl. Sci.* **2023**, *13*, 5561; f) J. E. López-Hernández, N. Nayeem, J. P. Cerón-Carrasco, A. Lahad, A. Hafeed, I. E. León, M. Contel, *Chem. Eur. J.* **2023**, *29*, e202302045; g) N. Curado, N. Giménez, K. Miachin, M. Aliaga-Lavrijsen, M. Cornejo, A. A. Jarzęcki, M. Contel, *ChemMedChem* **2019**, *14*, 1086–1095.
[10] a) J. E. López-Hernández, M. Contel, *Curr. Opin. Chem. Biol.* **2023**, *72*, 102250; b) B. Bertrand, A. Citta, I. L. Franken, M. Picquet, A. Folda, V. Scalcon, M. P. Rigobello, P. L. Gendre, A. Casini, E. Bodio, *J. Biol. Inorg. Chem.* **2015**, *20*, 1005–1020.
[11] a) J. Banfic', A. A. Legin, M. A. Jakupec, M. Galanski, B. K. Keppler, *Eur. J. Inorg. Chem.* **2014**, *2014*, 484–492;b) K. Mitra, U. Basu, I. Khan, B. Maity, P. Kondaiah, A. R. Chakravarty, *Dalton Trans.* **2014**, *43*, 751–763; c) P. Govender, H. Lemmerhirt, A. T. Hutton, B. Therrien, P. J. Bednarski, G. S. Smith, *Organometallics* **2014**, *33*, 5535–5545; d) C. M. Anderson, S. S Jain, L. Silber, K. Chen, S. Guha, W. Zhang, E. C. McLaughlin, Y. Hu, J. M. Tanski, *J. Inorg. Biochem.* **2015**, *145*, 41–50; e) C. Mu, S. W. Chang, K. E. Prosser, A. W. Y. Leung, S. Santacruz, T. Jang, J. R. Thompson, D. T. T. Yapp, J. J. Warren, M. B. Bally, T. V. Beischlag, C. J. Walsby, *Inorg. Chem.* **2016**, *55*, 177–190; f) N. K. Verma, A. Sadeer, A. Kizhakeyil, J. H. Pang, Q. Y. A. Chiu, S. W. Tay, P. Kumar, S. A. Pullarkat, *RSC Adv.* **2018**, *8*, 28960–28968; g) D. Aucamp, S. V. Kumar, D. C. Liles, M. A. Fernandes, L. Harmse, D. I. Bezuidenhout, *Dalton Trans.* **2018**, *47*, 16072–16081; h) T. A. C. A. Bayrakdar, T. Scattolin, X. Ma, S. P. Nolan, *Chem. Soc. Rev.* **2020**, *49*, 7044–7100.
[12] a) W. D. J. Tremlett, T. Söhnel, J. D. Crowley, L. J. Wright, C. G. Hartinger, *Inorg. Chem.* **2023**, *62*, 3616–3628; b) A. S. Braegelman, M. J. Webber, *Theranostics* **2019**, *9*, 3017–3040.
[13] a) A. Van Niekerk, P. Chellan, S. F. Mapolie, *Eur. J. Inorg. Chem.* **2019**, *2019*, 3432–3455; b) A. P. M. Guedes, F. Mello-Andrade, W. C. Pires, M. A. M. De Sousa, P. F. F. Da Silva, M. Camargo, H. Gemeiner, M. A. Amauri, C. G. Cardoso, P. R. De Melo Reis, E. De Paula Silveira-Lacerda, A. A. Batista, *Metallomics* **2020**, *12*, 547–561.
[14] a) T. Scattolin, V. A. Voloshkin, F. Visentin, S. P. Nolan, *Cell Rep. Phys. Sci.* **2021**, *2*, 100446; b) A. R. Kapdi, I. J. S. Fairlamb, *Chem. Soc. Rev.* **2014**, *43*, 4751–4777; c) T. Scattolin, I. Pessotto, E. Cavarzerani, V. Canzonieri, L. Orian, N. Demitri, C. Schmidt, A. Casini, E. Bortolamiol, F. Visentin, F. Rizzolio, S. P. Nolan, *Eur. J. Inorg. Chem.* **2022**, *2022*, e202200103; d) M. N. Alam, F. Huq, *Coord. Chem. Rev.* **2016**, *316*, 36–67; e) T. Scattolin, E. Bortolamiol, I. Caligiuri, F. Rizzolio, N. Demitri, F. Visentin, *Polyhedron* **2020**, *186*, 114607; f) T. Scattolin, E. Bortolamiol, F. Rizzolio, N. Demitri, F. Visentin, *Appl. Organomet. Chem.* **2020**, *34*, e5876; g) F. Huq, H. Tayyem, P. Beale, J. Q. Yu, *J. Inorg. Biochem.* **2007**, *101*, 30; h) J. Spencer, A. Casini, O. Zava, R. P. Rathnam, S. K. Velhanda, M. Pfeffer, S. K. Callear, M. B. Hursthouse, P. J. Dyson, *Dalton Trans.* **2009**, 10731; i) S. Ray, R. Mohan, J. K. Singh, M. K. Samantaray, M. M. Shaikh, D. Panda, P. Ghosh, *J. Am. Chem. Soc.* **2007**, *129*, 15042; j) T.-H. Fong, C.-N. Lok, C. Y.-S. Chung, Y.-M. E. Fong, P.-K. Chow, P.-K. Wan, C.-M. Che, *Angew. Chem. Int. Ed.* **2016**, *55*, 11935; k) X.-Q. Zhou, P. Wang, V. Ramu, L. Zhang, S. Jiang, X. Li, S. Abyar, P. Papadopoulou, Y. Shao, L. Bretin, M. A. Siegler, F. Buda, A. Kros, J. Fan, X. Peng, W. Sun, S. Bonnet, *Nat. Chem.* **2023**, *15*, 980–987; l) X.-Q. Zhou, M. Xiao, V. Ramu, J. Hilgendorf, X. Li, P. Papadopoulou, M. A. Siegler, A. Kros, W. Sun, S. Bonnet, *J. Am. Chem. Soc.* **2020**, *142*, 10383–10399; m) T. Scattolin, E. Bortolamiol, F. Visentin, S. Palazzolo, I. Caligiuri, T. Perin, V. Canzonieri, N. Demitri, F. Rizzolio, A. Togni, *Chem. Eur. J.* **2020**, *26*, 11868–11876; n) T. Scattolin, G. Moro, A. Serena, A. Guadagnin Pattaro, F. Rizzolio, V. Canzonieri, N. Demitri, E. Bortolamiol, L. M. Moretto, F. Visentin, *Appl. Organomet. Chem.* **2022**, *36*, e6629; o) T. Scattolin, S. Giust, P. Bergamini, I. Caligiuri, L. Canovese, N. Demitri, R. Gambari, I. Lampronti, F. Rizzolio, F. Visentin, *Appl. Organomet. Chem.* **2019**, *33*, e4902; p) T. Scattolin, I. Caligiuri, N. Mouawad, M. El Boustani, N. Demitri, F. Rizzolio, F. Visentin, *Eur. J. Med. Chem.* **2019**, *179*, 325–334; q) T. Scattolin, N. Pangerc, I. Lampronti, C. Tupini, R. Gambari, L. Marvelli, F. Rizzolio, N. Demitri, L. Canovese, F. Visentin, *J. Organomet. Chem.* **2019**, *899*, 120857; r) E. Bortolamiol, F. Fama, Z. Zhang, N. Demitri, L. Cavallo, I. Caligiuri, F. Rizzolio, T. Scattolin, F. Visentin, *Dalton Trans.* **2022**, *51*, 11135–11151; s) E. Bortolamiol, G. Isetta, I. Caligiuri, N. Demitri, S. Paganelli, F. Rizzolio, T. Scattolin, F. Visentin, *Eur. J. Inorg. Chem.* **2023**, *26*, e202300084.
[15] T. Scattolin, E. Cavarzerani, D. Alessi, M. Mauceri, E. Botter, G. Tonon, I. Caligiuri, O. Repetto, U. Kamensek, S. K. Brezar, M. Dalla Pozza, S. Palazzolo, M. Cemazar, V. Canzonieri, N. Demitri, S. P. Nolan, G. Gasser, F. Visentin, F. Rizzolio, *ChemRxiv.* **2024**, DOI: 10.26434/chemrxiv-2024-bd942.
[16] a) L. Canovese, F. Visentin, T. Scattolin, C. Santo, V. Bertolasi, *J. Organomet. Chem.* **2016**, *808*, 48–56; b) L. Canovese, F. Visentin, T. Scattolin, C. Santo, V. Bertolasi, *Polyhedron* **2016**, *113*, 25–34; c) L. Canovese, C. Santo, T. Scattolin, F. Visentin, V. Bertolasi, *J. Organomet. Chem.* **2015**, *794*, 288–300; d) F. Visentin, C. Santo, T. Scattolin, N. Demitri, L. Canovese, *Dalton Trans.* **2017**, *46*, 10399–10407.
[17] T. Scattolin, F. Visentin, C. Santo, V. Bertolasi, L. Canovese, *Dalton Trans.* **2016**, *45*, 11560–11567.
[18] T. Scattolin, M. Mauceri, N. Demitri, F. Rizzolio, F. Visentin, *Eur. J. Inorg. Chem.* **2024**, DOI: 10.1002/ejic.202400303.
[19] X. Zhao, C. Zhang, *Synthesis* **2007**, *2007*, 551–557.
[20] A. Lausi, M. Polentarutti, S. Onesti, J. R. Plaisier, E. Busetto, G. Bais, L. Barba, A. Cassetta, G. Campi, D. Lamba, A. Pifferi, S. C. Mande, D. D. Sarma, S. M. Sharma, G. Paolucci, *Eur. Phys. J. Plus* **2015**, *130*, 43.
[21] W. Kabsch, *Acta Crystallogr. D Biol. Crystallogr.* **2010**, *66*, 125–132.
[22] J. Agirre, M. Atanasova, H. Bagdonas, C. B. Ballard, A. Baslé, J. Beilsten-Edmands, R. J. Borges, D. G. Brown, J. J. Burgos-Mármol, J. M. Berrisford, *Acta Crystallogr. Sect. Struct. Biol.* **2023**, *79*, 449–461.
[23] P. R. Evans, G. N. Murshudov, *Acta Crystallogr. D Biol. Crystallogr.* **2013**, *69*, 1204–1214.
[24] G. M. Sheldrick, *Acta Crystallogr. Sect. A* **2015**, *71*, 3.
[25] G. M. Sheldrick, *Acta Crystallographica Section c* **2015**, *71*, 3.
[26] A. L. Spek, *Acta Crystallogr. Sect. C Struct. Chem.* **2015**, *71*, 9–18.
[27] P. Emsley, B. Lohkamp, W. G. Scott, K. Cowtan, *Acta Crystallogr. D Biol. Crystallogr.* **2010**, *66*, 486–501.
[28] L. J. Farrugia, *J. Appl. Crystallogr.* **2012**, *45*, 849–854.
[29] L. Schrodinger, *The PyMOL Molecular Graphics System.* Schrodinger, **2015**, LLC. http://www.pymol.org.

Manuscript received: June 2, 2024
Revised manuscript received: August 26, 2024
Accepted manuscript online: August 27, 2024
Version of record online: October 22, 2024